Radio Science, Volume 25, Number 5, Pages 961–973, September–October 1990

Computer processing for deriving drop-size distributions and vertical air velocities from VHF Doppler radar spectra

Toru Sato, Hiroshi Doji,[1] *Hisato Iwai,*[2] *and Iwane Kimura*

Department of Electrical Engineering II, Faculty of Engineering, Kyoto University, Kyoto, Japan

Shoichiro Fukao, Mamoru Yamamoto, Toshitaka Tsuda, and Susumu Kato

Radio Atmospheric Science Center, Kyoto University, Uji, Kyoto, Japan

(Received May 31, 1989; revised September 30, 1989; accepted October 11, 1989.)

A fully automated data processing procedure has been developed for deriving the precipitation parameters from VHF Doppler radar spectra simultaneously with the background atmospheric parameters such as the mean wind velocity. The procedure has largely enhanced our capability in analyzing the data from continuous observations, which was hardly possible with human-attained analysis. The accuracy of the derived parameters are quantitatively evaluated by means of numerical simulations. It is found that the rain parameters can be determined with an accuracy of 15% at a time and height resolution of 10 min and 600 m, respectively, for high signal-to-noise ratios, for example. Parameters for the background atmospheric turbulence are estimated with an accuracy more than twice the fitting procedure currently used to analyze clear-air data. Experimental results of the MU radar observations are compared with the rain intensity measured on the ground for the first time. It is confirmed that the radar has a capability of measuring rain parameters with a rainfall rate sensitivity of about 1 mm h^{-1}.

1. INTRODUCTION

Drop-size distribution is one of the most important parameters which is closely related to the nature of the precipitation event under observation, especially, since its height profile gives essential information concerning the generation process of the event.

Historically, the drop-size distribution has been one of the most important parameters to be determined in the field of microwave weather radars, since the relation between the received echo power from precipitation and the rainfall rate is largely affected by the size of drops. Conventional single-parameter radars, which can measure only the echo power, had to rely on empirical formulas which express the rainfall rate in terms of the reflectivity. The accuracy of estimates naturally depended on whether or not the precipitation event of interest has similar characteristics to those of the model data used in determining such formulas.

Multiparameter radars, such as dual-wavelengths radars or dual-polarization radars, which have a capability of deriving independent information about the drop-size distribution together with the reflectivity, have been developed to overcome this difficulty. Doppler weather radars have a large advantage of being able to determine the drop-size distribution directly from the observed echo power spectra, although it was necessary to subtract additional Doppler shifts as a result of background winds. Dual-Doppler radars have been used to measure the vector wind field simultaneously with the drop-size distribution.

Readers are referred to the works of *Doviak and Zrnić* [1984] for the principles and techniques of various types of weather radars developed for precipitation measurements. Intensive efforts have been paid to improve dual-polarization radars as reviewed by *Ulbrich* [1986], since they have an advantage of deriving two parameters of a target volume with a single antenna, while dual-wavelength radars may require two antennas in order to match the size of target volumes measured by the two wavelengths. Recent advances in data process-

[1] Now at Yamato Laboratory, IBM Japan Ltd., Yamato, Japan.

[2] Now at Kokusai Denshin Denwa Co. Ltd., Tokyo, Japan.

Paper number 89RS03243.
0048-6604/90/89RS-03243$08.00

ing schemes of dual-polarization radars and of dual-wavelength radars [e.g., *Sachidananda and Zrnić*, 1987; *Fujita et al.*, 1989] have shown substantial improvements in their comparisons of rainfall rates measured by the radars and by ground-based rain gauges.

In parallel to these developments in microwave weather radars it has been found that a sensitive VHF Doppler radar can detect precipitation echoes simultaneously with echo from the ambient atmosphere [*Fukao et al.*, 1985]. *Wakasugi et al.* [1986, 1987] investigated a computer algorithm to derive parameters of drop-size distribution as well as the mean vertical velocity and fluctuations due to turbulence from the radar spectra. Namely, assuming an exponential form which was suggested by *Marshall and Palmer* [1948] for the drop-size distribution and a Gaussian distribution for the atmospheric turbulence spectra, they have applied least squares fitting to the observed spectra. This method gives rise to reasonable parameters, in case good initial values are used for the parameters to be estimated.

The major advantage of using a VHF Doppler radar is that it is possible, in principle, to subtract all effects of background motion of the atmosphere on the derived drop-size distribution from a single measurement. While the significance of removing the mean wind velocity in the Doppler spectra has been recognized widely, the importance of removing various factors which cause spectral broadening, such as turbulence motion, beam broadening or shear broadening, does not seem to have been understood as widely. Effects of these broadening factors on the spectral width of radar echoes are discussed by *Hocking* [1983] in relation to the estimates of turbulence parameters from the spectral width.

Since these broadening factors largely depend on the beam width and the range resolution of the radar, it is very important to make these parameters equal when the precipitation spectrum and the background air motion are measured by different radars. Use of a VHF Doppler radar avoids such complication in experimental designs, although with an expense of a lower sensitivity to rain drops compared to microwave radars.

In the present paper we report the results of our study to extend the method developed by *Wakasugi et al.* [1986, 1987] to find appropriate initial parameters purely by computer in order to enable us to deduce the drop-size distribution and vertical atmospheric velocity automatically from original data. We have also improved their method by stabilizing the iterative solution when the fitting process is highly nonlinear and by giving constraints to the parameters to be changed.

We evaluate the accuracy of the derived parameters by means of numerical simulations. Echo power spectra are generated according to a set of model parameters, the background noise and random statistical fluctuations are added, then analyzed by the procedure developed here. The simulation is repeated for different random numbers to examine the variance of the derived parameters from the given ones.

Finally, we compare the rainfall rate derived from a series of observations made with the middle and upper atmosphere (MU) radar during a precipitation event with that measured on the ground at the MU radar site.

The technique we develop here is basically applicable to the Doppler spectra measured with microwave radars as well, since the spectral shape of the precipitation component does not depend on the radar frequency. Also, statistical fluctuations and thus the errors in the estimates of precipitation parameters have the same characteristics at different frequencies. Recently, *Currier and Avery* [1988] have developed a precipitation measurement system which consists of two Doppler radars operating at 50 MHz and 915 MHz. Their approach makes an efficient use of high sensitivity of UHF band to the rain drops combined with the capability of a 50-MHz wind profiler. Our procedure can be used in fitting the precipitation spectra measured by the UHF system based on the information of background atmosphere measured by the VHF system, if a sufficient care is paid to match the beam width and size of scattering volumes of the two systems.

It should be noted that any attempt using a VHF wind profiler as a reference of atmospheric motion should consider the effect of precipitation component on the observed spectra under medium-to-strong precipitation conditions because conventional spectral moments may be largely biased for such cases.

2. DOPPLER SPECTRA DUE TO ATMOSPHERIC TURBULENCE AND PRECIPITATION

The Doppler velocity spectrum $S_p(v)$ of echo due to precipitation by a vertical radar beam in the

condition without atmospheric turbulence and wind, is expressed in terms of the diameter of rain drops D as

$$S_p(v) = C \cdot N(D) D^6 \left| \frac{d[v(D)]}{dD} \right|^{-1} \quad (1)$$

where $N(D)dD$ is the number of particles with diameter between D and $D + dD$, $v(D)$ is the drop fall velocity measured as positive for upward direction for the drop-size D, and C is a constant. The explicit relation between D and v is given later in (8).

On the other hand, the Doppler spectrum $S_t(v)$ due to atmospheric turbulence by a vertical radar beam is approximated by the following Gaussian function,

$$S_t(v) = P_o \exp\left[-\frac{(v-w)^2}{2\sigma^2} \right] \quad (2)$$

where w is the mean wind velocity in the radar beam direction and σ is the spectral broadening.

If the rain drops completely follow the motion of atmospheric turbulence, the observed Doppler spectrum $S(v)$ due to the rain drop and atmospheric turbulence is expressed by

$$S(v) = S_t(v) + S_p(v) * S_o(v) + P_n \quad (3)$$

where $S_o(v)$ is a normalized form of $S_t(v)$, as follows:

$$S_o(v) = \frac{1}{(2\pi)^{1/2}\sigma} \exp\left[-\frac{(v-w)^2}{2\sigma^2} \right] \quad (4)$$

P_n in (3) is the noise level on the spectra. The asterisk denotes the convolution operation. However, because of the finite length of data for fast Fourier transform (FFT) analyses, the observed Doppler spectra actually obtained as a result of FFT are distorted by the window function $W(v)$ in such a way as

$$S'(v) = S(v) * W(v) \quad (5)$$

where $W(v)$ is an inverse Fourier transform of a triangular auto-correlation function of the boxcar time window. The theoretically estimated spectrum $S'(v)$ contains the information of drop-size distribution of precipitation as well as the atmospheric turbulence. In order to deduce this hidden information from the observed spectra a spectral fitting method was devised by *Wakasugi et al.* [1986, 1987], which is to find a parameter set that minimizes the difference ε defined by

$$\varepsilon = \sum_{i=1}^{N_{FFT}} [S_{obs}(v_i) - S'(v_i)]^2 \quad (6)$$

where v_i's are discrete velocity points corresponding to ith discrete frequency of FFT and N_{FFT} is the number of fitted points in the periodogram.

Their method works very well in deriving the precipitation parameters when a good initial guess for the parameters is provided. The largest restriction of their method is that the initial guess should be given manually, which prevented the application of the algorithm to a large volume of data. In the following section we describe our procedure for finding the initial guess fully automatically. However, as we will see later, it is not always easy to find a correct set of initial parameters by a computer algorithm. We therefore had to improve the fitting procedure itself so that it becomes more tolerant to bad initial parameters. We introduce a couple of numerical techniques known to be effective in stabilizing the nonlinear least square fitting procedure, namely, the modified Marquardt method and the penalty function method.

3. PARAMETER ESTIMATION PROCEDURE

3.1. *Identification of precipitation echo*

Since the nonlinear least squares fitting procedure described below is heavily time consuming, we first examine the Doppler spectra to check whether they contain the spectral component as a result of precipitation or not. Simply, this is to find twin peak on the spectra.

We first take logarithm of the spectral intensity to get 10 log $[S_{obs}(v_i)]$ and approximate it by polynominals $F_o(v_i)$ using the least squares method. The reason for taking the logarithm is that the magnitude of statistical fluctuations, which is proportional to the amplitude of the power spectra, is uniform versus frequency in the log-domain. Since the minimum level of the spectra is of the order of noise level P_n, the approximation by polynomial is made only within the frequency range satisfying

$$10 \log [S_{obs}(v_i)] - 10 \log P_n \geq 3 \quad (7)$$

The polynomial $F_o(v_i)$ to satisfy the above condition is realized by those including up to the 13th-order term. The reason for taking up to such higher-order terms is to closely fit the atmospheric turbulence component in order to pick up the precipitation component, which is often just a small bump in the atmospheric turbulence component.

To find a peak on the spectra, we calculate the first and second derivatives of the approximated function $F_o(v_i)$. By these processes a precipitation component as well as an atmospheric component can be simultaneously identified.

3.2. *Selection of initial values for nonlinear least squares fitting*

After identification of the echo from precipitation, we proceed to the step for estimation of drop-size distribution. For this procedure we can use the following well-known relation between drop-size D (millimeters) and drop fall velocity v(meters per second) [*Gunn and Kinzer*, 1949],

$$v(D) = -[9.65 - 10.3 \exp(-0.6D)] \cdot (\rho_o/\rho)^{0.4} \tag{8}$$

where ρ_o and ρ are the air densities at ground level and the level of observation aloft, respectively. This equation is however valid only for D larger than $D_{\min}$ that is the diameter to make the above $v(D)$ zero, that is

$$D_{\min} = -\ln(9.65/10.3)/0.6 = 0.11 \text{ mm} \tag{9}$$

In the following analysis we assume that there is no rain drop which has the drop-size smaller than $D_{\min}$. Actually the strength of scattering from rain drops is proportional to D^6, so that the contribution to the echo from smaller-sized particles becomes negligible at VHF, even taking the effect of an exponential increase in the number density at smaller sizes into account. Actually, at the smallest end of the size distribution where the drop fall velocity becomes much smaller than the wind velocity fluctuations due to atmospheric turbulence, the droplets show no detectable mean motion relative to the background air. In this region, scattering from the droplets simply enhances the magnitude of the atmospheric turbulence component in the observed echo power spectrum. Therefore the above assumption is reasonably valid.

On the other hand, as to the drop-size distribution, the following Marshall-Palmer distribution will be used,

$$N(D) = N_o \exp(-\Lambda D) \tag{10}$$

In the recent studies a more general form of the gamma distribution, which contains an additional D^{μ} factor in the right-hand side of (10), has often been used in order to take the variability of the Doppler spectra into account [*Ulbrich*, 1983]. We do not take this approach here because introducing an extra term slightly improves the fitting itself because of the increased freedom but significantly increases errors in the estimates of each parameter. It is because the μ term mainly affects the Doppler spectra at the small drop-size part with small Doppler velocities, which is usually masked by the strong turbulence component existing around the zero Doppler frequency in the VHF radar echoes. Small changes in the spectral shape of the precipitation component due to the μ term cannot therefore be distinguished from those due to the turbulence component.

It is known that for D larger than 6 mm, rain drops cannot stably exist, so they are broken into smaller sized particles. Therefore in the following analyses we assume that there is an upper limit for D in using (10), which will be denoted by $D_{\max}$. The maximum drop fall velocity $V_{\max}$ is determined from (8). $N(D)$ is now represented by

$$\begin{aligned} &N(D) = N_o \exp(-\Lambda D) && w + V_{\max} \le v \le w \\ &N(D) = 0 && v < w + V_{\max},\ w < v \end{aligned} \tag{11}$$

The parameters to be obtained by the fitting are P_o, w, σ, N_o, Λ, $V_{\max}$ and P_n. In order to use a nonlinear fitting algorithm, initial values for these seven parameters are required. For the initial value of P_n, the noise level defined in section 3.1 is used. The initial values for P_o, w, and σ are estimated from the observed spectra by taking moments of the 0th, 1st, and 2nd degree for a part of the spectrum corresponding to atmospheric turbulence.

For the three parameters N_o, Λ, and $V_{\max}$ it is rather difficult to reasonably estimate their initial values. We therefore select N_r different values for each parameters as the initial values, and we calculate ε to find its minimum among all combinations of these three parameters. Since the number of combinations amounts to N_r^3, computer time increases tremendously if N_r is large. In our trial we have

TABLE 1. Set of Initial Values for the Precipitation Component Used in the Fitting Procedure

	$N_0 = 100.0$	$N_0 = 1000.0$	$N_0 = 10000.0$
Λ (cm^{-1})	15.0	25.0	35.0
V_{max} (ms^{-1})	−9.0	−8.0	−7.0

found that $N_r = 3$ is a reasonable choice. The values selected for our calculation are listed in Table 1.

3.3. *Numerical procedure for the least squares fitting*

By using the initial parameters determined by the processes mentioned above, the theoretical Doppler spectrum $S'(v)$ is calculated. If there is no echo from rain drops, the following expression instead of (5) is used in order to estimate parameters for the atmospheric turbulence echo

$$S'(v) = [S_t(v) + P_n] * W(v) \tag{12}$$

From $S'(v_i)$ and the observed spectrum $S_{obs}(v_i)$, the square of the difference is calculated.

In the process of minimizing the error defined by (6) it is better to limit the range of frequency points from i_{fs} to i_{fe} defined below:

$$\begin{aligned} i_{fs} &= j_{pp} - 20 \\ i_{fe} &= j_{pt} + 20 \end{aligned} \tag{13}$$

for coexistence of raindrop echo and turbulence echo.

$$\begin{aligned} i_{fs} &= j_{pt} - 10 \\ i_{fe} &= j_{pt} + 10 \end{aligned} \tag{14}$$

for turbulence echo only, where j_{pp} and j_{pt} correspond to frequency points where precipitation echo and air turbulence echo, respectively, show maxima. In the above range the data point at zero Doppler shift ($i = N_{FFT}/2+1$) is also removed in order to reduce a clutter effect. Namely, the error to be minimized is

$$\varepsilon = \sum_{i=ifs(i \neq N_{FFT}/2+1)}^{ife} \{\log [S_{obs}(v_i)] - \log [S'(v_i)]\}^2 \tag{15}$$

As an algorithm for minimization of ε, the nonlinear least squares fitting method is used as follows.

We denote

$$\begin{aligned} \mathbf{X} &= (P_o, w, \sigma, N_o, \Lambda, V_{max}, P_n)^T \\ \mathbf{Y} &= (Y_1, Y_2, \cdots, Y_{N_{FFT}})^T \\ Y_i &= \log [S_{obs}(v_i)] \\ \mathbf{f}(\mathbf{X}) &= [f_1(\mathbf{X}), f_2(\mathbf{X}), \cdots, f_{N_{FFT}}(\mathbf{X})]^T \\ f_i(\mathbf{X}) &= \log [S'(v_i)] \\ (i &= 1\text{–}N_{FFT}) \end{aligned} \tag{16}$$

where the superscript T means to transpose. In case that there is no precipitation echo

$$\mathbf{X} = (P_o, w, \sigma, P_n)^T \tag{17}$$

We adopt iterative approach in finding the set of parameters $\mathbf{X}$ which provides the minimum value of ε. Let us consider a method to improve the kth estimate of $\mathbf{X}^k$, starting from the original value of $\mathbf{X}^o$, which is determined by the way as discussed in the previous section. A Taylor expansion of $f_i(\mathbf{X})$ in the vicinity of $\mathbf{X}^k$, results in

$$f_i(\mathbf{X}) \simeq f_i(\mathbf{X}^k) + \left[\frac{\partial f_i(\mathbf{X})}{\partial \mathbf{X}}\right]_{X = X^{(k)}} \cdot (\mathbf{X} - \mathbf{X}^{(k)}) \tag{18}$$

where $\partial f_i(\mathbf{X})/\partial \mathbf{X}$ denotes a vector whose elements are $\partial f_i(\mathbf{X})/\partial X_j$, and X_j is jth element of $\mathbf{X}$. If we write

$$\begin{aligned} \Delta \mathbf{X}^k &= \mathbf{X} - \mathbf{X}^{(k)} \\ \Delta \mathbf{Y}^k &= \mathbf{Y} - \mathbf{f}[\mathbf{X}^{(k)}] \end{aligned}$$

then using (18) we obtain

$$\Delta \mathbf{Y}^{(k)} = \mathbf{A} \Delta \mathbf{X}^{(k)} \tag{19}$$

where $\mathbf{A}$ is a Jacobian matrix whose elements denote first order derivatives:

$$A_{ij} = \frac{\partial f_i[\mathbf{X}^{(k)}]}{\partial X_j} \tag{20}$$

We can obtain $\Delta \mathbf{X}^{(k)}$ by solving (19). However, it cannot be directly solved because the dimension of $\mathbf{Y}$ is the number of spectral points, which is larger than the dimension of $\mathbf{X}$, that is the number of parameters. We thereby have to reduce the dimension of (19) into that of $\mathbf{X}$ in order to solve it. While there is an arbitrariness in doing so, a set of least squares solution for $\Delta \mathbf{X}^{(k)}$ is obtained by solving the

following normal equation, which is uniquely given by taking partial derivatives of (15) to be zero.

$$\mathbf{A}^T\mathbf{A}\Delta\mathbf{X}^{(k)} = \mathbf{A}^T\Delta\mathbf{Y}^{(k)} \tag{21}$$

The next $\mathbf{X}^{(k+1)}$ is then obtained by

$$\mathbf{X}^{(k+1)} = \mathbf{X}^{(k)} + \Delta\mathbf{X}^{(k)} \tag{22}$$

By the repetition of this algorithm we can obtain a set of parameters which provides the best fit spectrum. This basic procedure has been used to analyze the MU radar data under precipitating conditions [*Wakasugi et al.*, 1987]. However, the solution of (20) turns out to be not always stable because of the nonlinearity in $\mathbf{f}(\mathbf{X})$. Here we apply the modified Marquardt method [e.g., *Fletcher*, 1979] to stabilize the solution by adding an extra term in the left-hand side of (20) as

$$(\mathbf{A}^T\mathbf{A} + \lambda\mathbf{I})\Delta\mathbf{X}^{(k)} = \mathbf{A}^T\Delta\mathbf{Y}^{(k)} \tag{23}$$

where λ is the modification factor determined from the nonlinearity of $\mathbf{A}^T\mathbf{A}$ in each step of iteration. The case $\lambda = 0$ is the Gauss-Newton method, and $\lambda = \infty$ corresponds to the steepest descent method.

This numerical procedure sometimes results in parameters with physically meaningless values, such as negative power or negative spectral index. In order to avoid this problem we introduced a penalty function method [e.g., *Bard*, 1974]. A penalty function takes a very large value for a prohibited region of $\mathbf{X}$ and decreases smoothly as the distance from the boundary increases. By adding this function to the right-hand side of (15) we can confirm that the solution is within the desired limit. The value of the penalty function is decreased as the iteration converges. A similar approach was employed by *Sato and Woodman* [1982] in the data analysis of clear-air radar echoes in the presence of fading clutter.

This iterative procedure is judged to have converged when condition 1, $\varepsilon < E$, or condition 2, $\Delta\varepsilon \leq (1 + \varepsilon) \cdot \varepsilon_f$ and $|\Delta X_j| \leq \varepsilon_{Xj} (j = 1, \cdots, 7)$, is satisfied, where E, ε_f, and ε_{xj} are thresholds which are empirically determined.

Although the above conditions are widely used as standard ones, the condition 2 is sometimes improperly satisfied when the given set of initial parameters is far from the right one, resulting in an "apparent convergence." For such a case, the modification factor λ in (23) becomes very large at an early stage of iterations because the variance function becomes highly nonlinear. In contrast, λ becomes very small when the procedure is working around the right set of parameters. We thereby introduce another condition to eliminate the data obtained from an apparent convergence. Namely, we abandon the data when condition 3, $\lambda_{\min} > \lambda_e$, is satisfied, where $\lambda_{\min}$ is the minimum value of λ in all iterations and λ_e is a proper threshold chosen as discussed in the following section, when a convergence is judged by conditions 1 and 2.

4. COMPUTER SIMULATION OF THE NONLINEAR LEAST SQUARES FITTING FOR DERIVING RAIN DROP-SIZE DISTRIBUTION

In order to assess the least squares fitting method described in the previous section, a computer simulation has been made. This simulation is based on the operation parameters of the MU radar listed in Table 2, which are used for standard tropospheric observations. The simulation procedure is similar to that used by *Yamamoto et al.* [1988] to evaluate the data processing procedure for the clear-air echoes observed by the MU radar.

A model echo power spectrum from precipitating atmosphere is generated according to (3) based on an appropriate set of parameters which are chosen from observed values. It is then smeared by (5) to take the effect of finite data length. Figure 1*a* shows an example of the theoretical echo power spectrum versus Doppler velocity. The left peak with a large negative Doppler velocity is due to precipitation, while the right peak is due to atmospheric turbulence component. Random statistical fluctuations are then added to the spectrum by multiplying the theoretical spectrum with a uniform spectrum having Gaussian random fluctuations as shown in Figure 1*b*, resulting in a spectrum as shown in Figure 1*c*. The purpose of multiplying is to represent the nature of the signal whose statistical fluctuation is proportional to the spectral density itself. The magnitude of fluctuation is proportional to $N_{\text{icoh}}^{-1/2}$ times the amplitude of the spectrum, where N_{icoh} is the number of incoherent integration, or temporal averaging of a series of N_{icoh} echo power spectra. Although the exact distribution of the fluctuation is given by a χ^2 distribution, it can be well approximated by a Gaussian when N_{icoh} is large. This model spectrum is then analyzed by the procedure as described above, and the resultant parameters

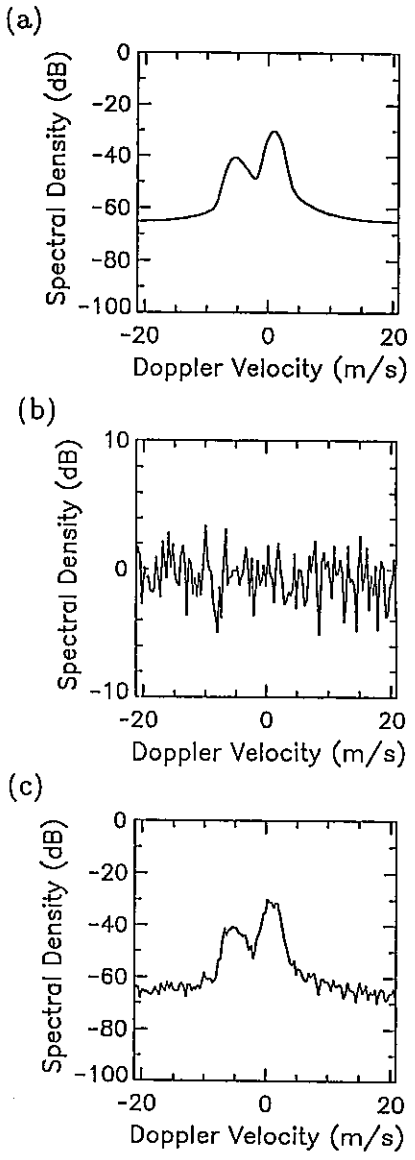

Fig. 1. An example of the model spectra used in the numerical simulation. (*a*) The theoretical spectra without statistical fluctuations (*b*) is multiplied by a uniform spectrum with random Gaussian fluctuations (*c*), resulting in the final model spectrum.

are compared with the given ones. The simulation is repeated 500 times for each set of the model parameters with different random numbers to remove statistical effects in the evaluation of errors.

We first examine errors in estimating three parameters, N_o, Λ, and $V_{\max}$, which represent precipitation characteristics among the seven parameters. Before presenting the result we examine the effect of apparent convergence discussed in the previous

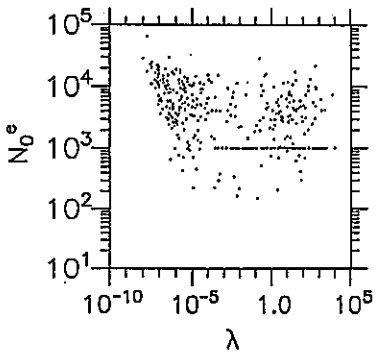

Fig. 2. Modification factor λ at the last iteration of fitting versus the estimated number density of rain drops N_o^e obtained from simulations with various model values of N_o and with $N_{\text{icoh}} = 6$.

section. Figure 2 plots, for example, the modification factor λ at the last iteration of fitting versus the estimated number density of rain drops N_o^e obtained from simulations with various model values of N_o and with $N_{\text{icoh}} = 6$. The superscript e denotes estimated values in the followings. It should be noted here that N_o has an arbitrary unit because the MU radar has no absolute calibration. Since the model values of N_o are given randomly in a wide range of 10^2–10^5 in this simulation, N_o^e should spread in this range as well. The horizontal line at $N_o^e = 10^3$, which is one of the initial values of N_o as given in Table 1, thus indicates that the simulation has incorrectly "converged" without modifying N_o from the given initial values at all.

If the linear expansion of the theoretical function as shown in (18) gives a good approximation of the observed spectra for a given set of parameters in an iteration, the variance should be a quasi-quadratic function of ΔX_j's. The Gauss-Newton method gives the correct answer for such a case with a few times of iterations. If not, the modified Marquardt method judges that the theoretical function is not expressing the data well, and it follows the steepest descent method, which is much less efficient than the Gauss-Newton method, but more stable. Small values of λ are thus desirable, because λ represents the local nonlinearity of the fitting, and a large λ means the fitting is not good at that iteration.

The wide range of spread of λ values, however, does not necessarily mean that the result of the fitting is bad. It was found that λ often takes a large value at final stages of iterations after the procedure finds the right location of minimum ε, if the ε

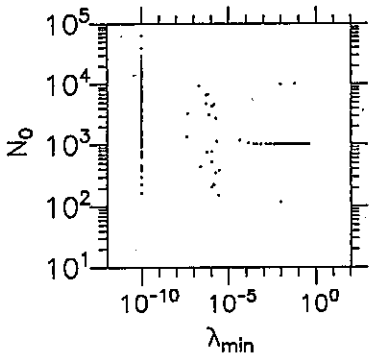

Fig. 3. Same as Figure 2, but the abscissa is for λ_{min} instead of final λ. The abscissa values smaller than 10^{-10} are represented by 10^{-10}.

surface has a flat bottom raised by random fluctuations of the spectrum.

Figure 3 plots λ_{min} versus N_o^e instead of final λ in Figure 2. Note that λ_{min} values smaller than 10^{-10} are represented by 10^{-10}. The cluster of points at such small values of λ_{min} means that pure Gauss-Newton method was chosen at least in one iteration by the procedure, which is a good indication that the procedure found the correct direction. Larger values of λ_{min} thereby means that the procedure never found the fitting proceeding smoothly, or it could not move from the given starting point. Because of this clear separation of the points, we can safely choose the threshold λ_e in condition 3 to be a small number as 10^{-9}.

As discussed before, the magnitude of statistical fluctuations in the spectra is a function of the number of incoherent integration, N_{icoh}, which determines the quality of fitting when the signal-to-noise ratio (snr) is large. Although the simulations are made for finite snr as well, we will limit our discussion here to the infinite snr case, because the snr is large enough for the altitude region where precipitation is observed, as far as the MU radar observations are concerned. Figure 4 shows examples of the quality of fitting. The left panels show the mean value of N_o, Λ, and V_{max} among 500 estimates, while the right panels show their standard deviations. The model values of the parameters are set to the center of each ordinate. The N_{icoh} values in the abscissa cover a range of 6–400, which correspond to time resolutions of 1 min to 1 hour, if no averaging is made with height (150-m height resolution).

Comparison of the left and right panels shows

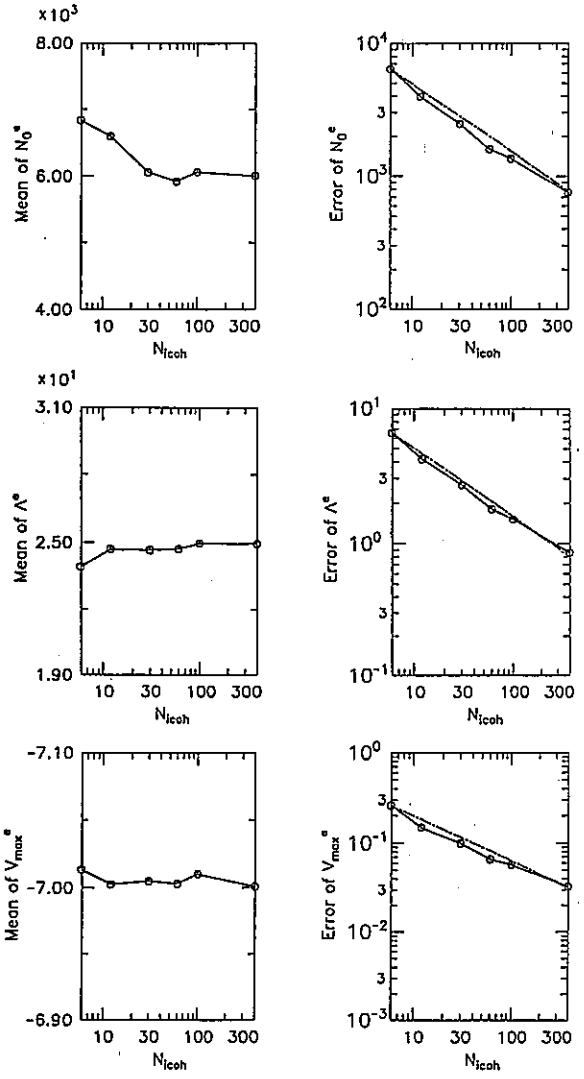

Fig. 4. The mean value of N_o, Λ, and V_{max} among 500 estimates (left panels) and their standard deviations (right panels). The model values of the parameters are set to the center of each ordinate. The dot-dash lines in the right panels indicate a slope of $N_{icoh}^{-1/2}$.

that the biases in the estimated parameters are very small, if any, compared to the standard deviations. On the other hand, the standard deviation of N_o^e is quite large, amounting to 100% for $N_{icoh} = 6$, which corresponds to the minimum time and height resolutions of 1 min and 150 m, respectively. The relative error in Λ seems to be smaller than that of N_o, but it turns out not to be so because Λ is a spectral index in the exponent, and its small change has a drastic effect on the shape of the spectrum.

The error in V_{max} is indeed small, probably because the cutoff point of a spectrum at the largest Doppler shift is clear even after smearing by (3) and (5).

The dot-dash lines in the right panels indicate a slope of $N_{icoh}^{-1/2}$. General agreement of the slope of the calculated curves with these lines indicates that the errors in the estimates are linearly proportional to the magnitude of statistical fluctuations in the spectra as is the case for linear least squares fitting. In order to obtain an accuracy of 15%, for example, we need to increase N_{icoh} to about 200. This number of incoherent integration is achieved by averaging the spectra or derived parameters over a period of 10 min and also over a height range of 600 m.

Although these resolutions may not be sufficient for some applications, better resolutions can be obtained only with an expense of larger errors. Use of a higher frequency than VHF is advantageous in this respect, since the short signal correlation time enables a large number of incoherent integration for a given duration. It should be noted, however, that for a given N_{icoh}, the observed Doppler spectra and thus derived parameters should contain the same amount of statistical errors regardless to the radar frequency and no matter how high the snr is. A sufficient care must be taken in interpreting the drop-size distribution measured by a radar so that the variability of observed Doppler spectra due to statistical fluctuations in the scattering process are not confused with the natural variability of the drop-size distribution. For example, if we analyze the same simulated spectra with 1-min resolution (N_{icoh} = 6) assuming a gamma distribution, large values of the index μ may result even though the model spectra is generated for μ = 0.

We next examine the accuracy of other parameters concerning atmospheric turbulence component, i.e., P_o, w, and σ. Figure 5 shows mean values and standard deviations of these parameters derived simultaneously with precipitation parameters shown in Figure 4. The model parameters are again given as the center values of the ordinates of the left panels. The echo power P_o has the same arbitrary unit as N_o. Comparison of this figure with Figure 4 clearly shows that the parameters for the atmospheric turbulence component is estimated with much higher accuracy than those for the precipitation component. The error of P_o, for example, is 15% with an incoherent integration of 6 times, in contrast to that of N_o of 100%. The line of sight velocity w is derived with an accuracy of 6 cm s^{-1}

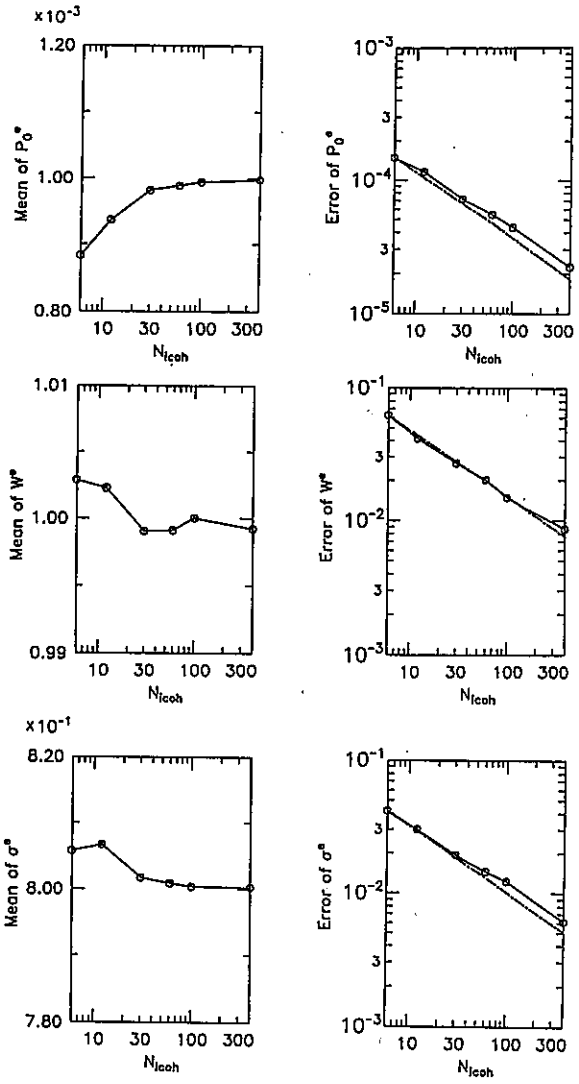

Fig. 5. Same as Figure 4, but for P_o, w, and σ derived simultaneously with precipitation parameters shown in Figure 4.

with N_{icoh} = 6, which is already high enough for most analyses.

Actually, the accuracy of the present procedure in deriving the parameters for the atmospheric turbulence component turned out to be higher than that of the standard nonlinear fitting procedure used routinely to analyze clear air echoes of the MU radar. Figure 6 compares the error of Doppler shift, which is equivalent to w, in a unit of frequency interval between the discrete spectral components Δf versus N_{icoh}. In the present case, Δf is 0.1 Hz, which corresponds to a line-of-sight velocity of 0.33 m s^{-1} as shown in Table 2. Lines with triangle,

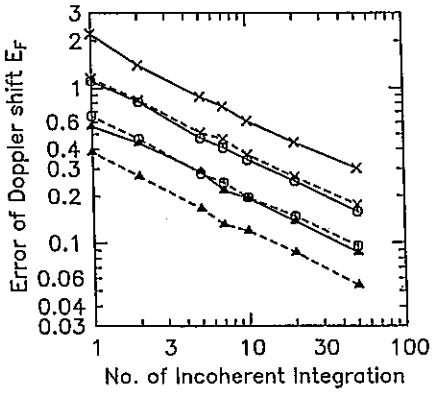

Fig. 6. Error of mean Doppler shift estimated by the standard fitting procedure used for the MU radar data analysis (solid lines) and by the present procedure. Lines with triangle, circle, and cross marks represent the case of $\sigma = \Delta f$, $3\Delta f$, and $10\Delta f$, respectively.

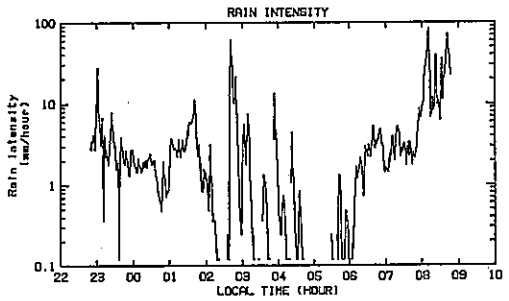

Fig. 7. Temporal variation of the rain intensity measured on the ground at the MU radar site by a drop-counter type rain gauge from 2200 LT, July 14 to 0900 LT, July 15, 1988.

circle, and cross marks represent the case of $\sigma = \Delta f$, $3\Delta f$, and $10\Delta f$, respectively. The solid lines denote the error of the standard procedure evaluated by a numerical simulation by *Yamamoto et al.* [1988], and the dashed lines are those of the present procedure. Clearly, the error of the present procedure is always smaller than that of the standard procedure by a factor of 1.5–2.0.

This improvement probably arises from the fact that we apply the nonlinear fitting procedure to the logarithm of the echo power spectrum, while the standard procedure fits in the linear domain. Yamamoto et al. pointed out that the fitting to the logarithm of the spectra is better because the magnitude of statistical fluctuations becomes independent of frequency. They showed that the fitting in the log domain yields an accuracy very close to the theoretical lower limit of the maximum likelihood estimates set by the Cramer-Rao bound for an ideal situation of no spectral distortion due to (5). Our estimates are still worse than the Cramer-Rao bound by a factor of about 5 for $\sigma = 10\Delta f$, and by a factor of 200 for $\sigma = \Delta f$. This difference is most likely due to the spectral distortion by (5), whose effect is more serious for narrower spectra than for broader ones.

Although still far from the theoretical lower limit of the error, it has been shown that our procedure fits the model spectra very well to the data spectra, even better than the standard procedure, at least to the atmospheric turbulence component. Since the fitting is made for the seven parameters as a whole and since the variance of the fitting does not depend on the presence of the precipitation component, we can assess that the curve fitting itself is working properly. The reason for higher errors in the derived precipitation parameters apparently arises from the insensitivity of the spectra to the parameters of concern.

5. COMPARISON OF THE RAIN INTENSITY MEASURED BY THE MU RADAR AND BY A RAIN GAUGE

In order to examine the performance of the present data processing procedure we have applied it to the MU radar data taken during a precipitation event of a duration of 11 hours observed on July 14–15, 1988. Figure 7 shows the intensity of the rain measured by a rain gauge located at the MU radar site. The rain gauge is a drop-counting system with a sensitivity down to 0.1 mm h^{-1}, and recorded the drop counts every minute. The rain is basically stratiform type, associated with several convective activities typical to Bai-U (rainy season), when a stationary front stretches zonally across the Japan islands. The front was moving slowly to the north during the observation period and passed over the MU radar at around 0800 LT.

The MU radar operated with a standard troposphere observation mode as listed in Table 2. Figure 8 indicates the detection of echoes by the MU radar with the present data processing procedure. The procedure was applied to the observed spectra after six times of incoherent integration, resulting in parameters obtained with a time and height intervals of 1 min and 150 m, respectively. Large dots denote data points when both the precipitation and turbulence components are identified, and small

TABLE 2. Operational Parameters of the MU Radar for Tropospheric Observations

Parameter	Value
Location	Shigaraki, Shiga, Japan (34.85°N, 136.10°E)
Radar system	monostatic pulse radar; active phased array system
Operational frequency	46.5 MHz
Antenna	circular array of 475 crossed Yagi's
aperture	8330 m^2 (103 m in diameter)
beam switching	switched alternately every IPP among 5 directions
beam directions	vertical and north, east, south, and west directions at 10° zenith angle
peak power	1 MW (maximum)
IPP	400 μs
Pulse width	1 μs
Height resolution	150 m
Coherent integration	38 pulse cycles (1 cycle = 5 IPP's)
FFT points	128
Doppler window	$\pm$21.0 m s^{-1}
Frequency resolution	0.1 Hz (0.33 m s^{-1})
Incoherent integration	6 times (before fitting)
Time resolution	64 s

IPP is the interpulse period.

dots denote that only the turbulence component was detected. Blank area means whether the echo was too weak or the fitting procedure did not converge. Data below about 1.5 km is not reliable because of the reduced receiver sensitivity as a result of transmit-receive switching.

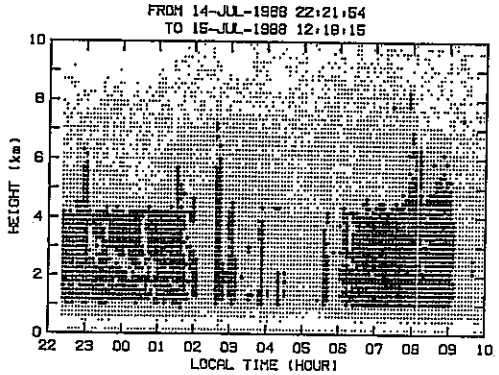

Fig. 8. Detection of echoes by the MU radar. Each dot corresponds to data taken at a time and height interval of 1 min and 150 m, respectively. Large dots denote data points when both the precipitation and turbulence components are identified, and small dots denote that only the turbulence component was detected. Data below about 1.5 km is not reliable because of the reduced receiver sensitivity due to transmit-receive switching.

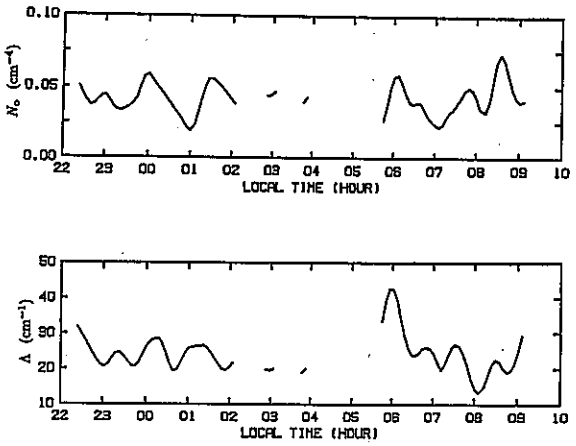

Fig. 9. Temporal variations of N_o calibrated by the rain gauge to the unit of cm^{-4} (top panel) and the spectral index Λ (cm^{-1}) (bottom panel). Parameters are averaged over 1.5–3.5 km altitude range, and applied 10-min running average.

Most of the precipitation data observed here are liquid water as judged from v_{max} values and detected below the height of 4.5 km, where the temperature exceeds 0°C. During several convective activities such as seen at around 2250, 0140, 0240, and 0800 LT, rain drops were detected up to a few kilometers above the freezing altitude, suggesting the occurrence of super cooling. By comparing Figures 7 and 8, we find that the MU radar has a sensitivity of detecting rain drops under a rainfall rate of about 1 mm h^{-1} or slightly less.

Since the MU radar does not have an absolute calibration for the echo power, we cannot directly convert N_o into the liquid water content. Here we normalize the data via the rain intensity measured on the ground averaged from 2300 LT to 0200 LT, when the rain was fairly steady. The mean effective rain intensity for the same period at an altitude range of 1.5–3.6 km, where the rain parameters are fairly stable, is calculated from the estimated drop-size distribution $N(D)$ through (10) with the uncalibrated unit and from the terminal velocity of drops $v(D)$ given by (8), and then compared to the mean rainfall rate on the ground. The same normalization factor thus determined is applied to the entire data set discussed here.

Figure 9 gives temporal variations of N_o normalized by this manner to the unit of cm^{-4} together with the spectral index $\Lambda(cm^{-1})$. Parameters are averaged over 1.5–3.6 km altitude range, and applied 10-min running average to reduce statistical

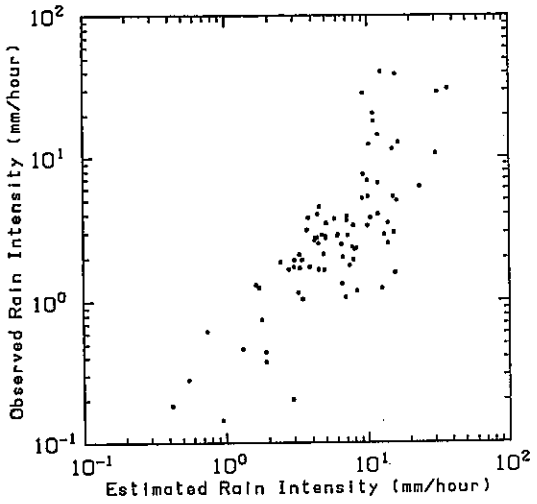

Fig. 10. Correlation diagram of the estimated rain intensity at an altitude range of 1.5–3.6 km by the MU radar and the rain intensity measured at the radar site by the rain gauge for the entire observation period. Each dot denotes an average over 10 min.

errors. The spectral index Λ is generally small, which means the drop size is large, for the period of convective activities when rain drops are observed above the 0°C height. It is especially clear for 0800 LT when the front passed over the radar. It should be noted that there is no enhancement in N_o for this period, showing that the enhancement observed in the rain intensity is caused mostly by growth of each rain drop. Some features as the large increase of N_o after 0800 LT or the sudden change of Λ at 0600 LT do not seem to have corresponding phenomena. More detailed comparisons with other meteorological parameters are required to explain this variability.

Figure 10 shows the correlation diagram of the estimated rain intensity at an altitude range of 1.5–3.6 km by the MU radar and the rain intensity measured at the radar site by the rain gauge for the entire observation period. Each dot denotes an average over 10 min. Since the rain drops take about 7 min on average to fall from the altitude region to the ground, a correction is made to compensate this delay. The correlation coefficient between the two rain intensities is 0.70. It should be noted here that this comparison is made for relatively light rain conditions, which may affect the specific value of the correlation coefficient.

There is a general tendency in this diagram that the rain intensity derived from the radar data is slightly larger than that of the rain gauge. This offset may mean that the normalization made above was not appropriate. As far as the present data is concerned, the offset can be easily corrected by adjusting the normalization factor based on this correlation diagram. Another explanation is that light precipitation evaporates more easily than heavy precipitation, so the comparison may be better for heavier rainfall rate. However, a more straightforward procedure, such as to establish an absolute calibration of the MU radar using the galactic noise level map, is desirable in any way for continuous observations.

It is not easy to separate various natural factors which deteriorate the correlation, such as the horizontal drifts of the rain area while falling from the altitude region to the ground and evaporation or growth of the rain drops within and below the region, from the statistical or systematic errors in the estimates. Although the simulation suggests that the difference between the ground and the radar measurements is too large to be attributed to the error in the estimates of rain parameters from the radar data alone, further comparisons including the ones with multipoint measurements of the rain intensity on the ground will be needed to confirm the total accuracy of the radar measurements.

6. SUMMARY

The capability of the large VHF Doppler radar in measuring the precipitation parameters was quantitatively evaluated. The data processing procedure has been fully automated by a combination of a new algorithm to find a set of initial guesses needed for the nonlinear least squares fitting procedure and with an improved fitting algorithm which includes a stabilization of the process by the modified Marquardt method and by the penalty function approach.

The accuracy of the procedure was quantitatively evaluated by means of numerical simulations. Statistical fluctuations were found to be the major factor in determining the accuracy of the estimates, and an accuracy of 15% was achieved for the precipitation parameters at a time and height resolution of 10 min and 600 m, respectively. The superior performance of the present procedure in analyzing the clear-air data over the currently used one was demonstrated.

A series of precipitation events observed by the MU radar was analyzed by the present procedure, and the result was compared with the rain intensity measured on the ground. The MU radar was found to have a sensitivity of measuring rain parameters at a rain intensity of about 1 mm h^{-1}.

REFERENCES

Bard, Y., *Nonlinear Parameter Estimation*, Academic, San Diego, Calif., 1974.

Currier, P. E., and S. K. Avery, Use of two wind profilers for precipitation studies, paper presented at Fourth Workshop on Technical and Scientific Aspects of MST Radar, Sci. Comm. on Sol. Terr. Phys., Kyoto, Japan, 1988.

Doviak, R. J., and D. S. Zrnić, *Doppler Radar and Weather Observations*, Academic, San Diego, Calif., 1984.

Fletcher, R., *Practical Methods of Optimization*, John Wiley, New York, 1979.

Fujita, M., K. Nakamura, H. Inomata, and K. Okamoto, Intercomparison of radar measurements of rain by single- and dual-wavelength techniques, *Radio Sci.*, *24*, 65–75, 1989.

Fukao, S., K. Wakasugi, T. Sato, S. Morimoto, T. Tsuda, I. Hirota, I. Kimura, and S. Kato, Direct measurement of air and precipitation particle motion by VHF Doppler radar, *Nature*, *316*, 712–714, 1985.

Gunn, R., and G. D. Kinzer, The terminal velocity of fall for water droplets in stagnant air, *J. Meteorol.*, *6*, 243–248, 1949.

Hocking, W. K., On the extraction of atmospheric turbulence parameters from radar backscatter Doppler spectra, 1, Theory, *J. Atmos. Terr. Phys.*, *45*, 89–102, 1983.

Marshall, J. S., and W. M. Palmer, The distribution of raindrops with size, *J. Meteorol.*, *5*, 165–166, 1948.

Sachidananda, M., and D. S. Zrnić, Rain rate estimates from differential polarization measurements, *J. Atmos. Oceanic Technol.*, *4*, 588–598, 1987.

Sato, T., and R. F. Woodman, Spectral parameter estimation of CAT radar echoes in the presence of fading clutter, *Radio Sci.*, *4*, 817–826, 1982.

Ulbrich, C. W., Natural variations in the analytical form of the raindrop size distribution, *J. Appl. Meteorol.*, *22*, 1764–1775, 1983.

Ulbrich, C. W., A review of the differential reflectivity technique of measuring rainfall, *IEEE Trans. Geosci. Remote Sens.*, *GE-24*, 955–965, 1986.

Wakasugi, K., A. Mizutani, M. Matsuo, S. Fukao, and S. Kato, A direct method for deriving drop-size distribution and vertical air velocities from VHF Doppler radar spectra, *J. Atmos. Oceanic Technol.*, *3*, 623–629, 1986.

Wakasugi, K., A. Mizutani, M. Matsuo, S. Fukao, and S. Kato, Further discussion on deriving drop-size distribution and vertical air velocities from VHF Doppler radar spectra, *J. Atmos. Oceanic Technol.*, *4*, 170–179, 1987.

Yamamoto, M., T. Sato, P. T. May, T. Tsuda, S. Fukao, and S. Kato, Estimation of spectral parameters of mesosphere-stratosphere-troposphere radars obtained by least squares fitting method and its lower bound, *Radio Sci.*, *23*, 1013–1021, 1988.

H. Doji, Yamato Laboratory, IBM Japan, Ltd., 1623-14 Shimo-Tsuruma, Yamato 242, Japan.

H. Iwai, Megura R&D Laboratories, Kokusai Denshin Denwa Co, Ltd., 2-1-23 Nakamegura, Megura-ku, Tokyo 153, Japan.

I. Kimura and T. Sato, Department of Electrical Engineering II, Faculty of Engineering, Kyoto University, Kyoto 606, Japan.

S. Fukao, S. Kato, T. Tsuda, and M. Yamamoto, Radio Atmospheric Science Center, Kyoto University, Uji, Kyoto 611, Japan.